Analyst

Accepted Manuscript

ROYAL SOCIETY OF CHEMISTRY

www.rsc.org/analyst

Journal Name

RSCPublishing

COMMUNICATION

Dual-Stimuli Responsive I-motif/Nanoflares for sensing ATP in Lysosome†

Cite this: DOI: 10.1039/x0xx00000x

Fen Jin,[ab] Jing Zheng,[a] Changhui Liu,[a] Sheng Yang,[a] Yinhui Li,[a] Jishan Li,[a] Yan Lian[a] and Ronghua Yang*[a]

Received 00th January 2014,
Accepted 00th January 2014

DOI: 10.1039/x0xx00000x

A dual-stimuli responsive i-motif/nanoflares for molecule detection in lysosome was designed. By combining structure-switchable i-motif sequence and high recognition ability of adenosine triphosphate (ATP) aptamer, subcellular sensing and visualization sensing of ATP in lysosome at the subcellular level can be achieved. This general sensing technique can be applied for a broad range of cellular communication studies to improve our understanding of subcellular signaling and function.

The distribution and dynamics of biological molecules inside cells are important to understand physiological processes, diagnose disease stages, and identify therapeutic targets.[1] In recent decades, much effort has been dedicated to developing chemosensors for biological molecules to elucidate their diverse physiological functions. However, location specificity, in particular lysosome analytes detection and imaging remains challenges because lysosome localization allows selective monitoring of biological events occurring in a specific region with high accuracy and low background. Subcellular imaging studies using small molecule-based chemosensors have been reported by several groups in recent years.[2] Most of these studies for subcellular imaging is to use fluorescent chemosensors that can spontaneously localize in a specific cellular region. This method is convenient and versatile because it does not require cumbersome protein expression or time-consuming protein maturation. Despite these advantages, but insufficient resolution in water and sophisticated synthesis of the probe materials, still existed. Thus, the number of autolocalizable fluorescent sensors suitable for subcellular bioimaging is limited.[3] Nevertheless, none of these probes is well suited for lysosomal applications, they can't specifically localize in lysosomes and monitor lysosomal ATP.

Recently, nucleic acid molecular probes as new kind of materials have been designed to image intracellular proteins, RNAs, small molecules and ions.[4] I-motif is a single-stranded DNA structure that forms due to intramolecular noncanonical base pair interactions between a protonated and an unprotonated cytosine residue under slightly acidic conditions.[5] The transition to the i-motif conformation, in which only half of the cytosines are protonated, takes place in the pH range between 6 and 7.[6] Coincidently, intracellular pH is generally between 6.8 and 7.4 in the cytosol and between 4.5 and 6.0 in the cell's acidic organelles such as lysosome.[7] Therefore, this i-motif switch recapitulates with high fidelity, its *in vitro* pH response inside cells, illustrated by the capture of spatio-temporal pH changes and subcellular such as lysosome location.

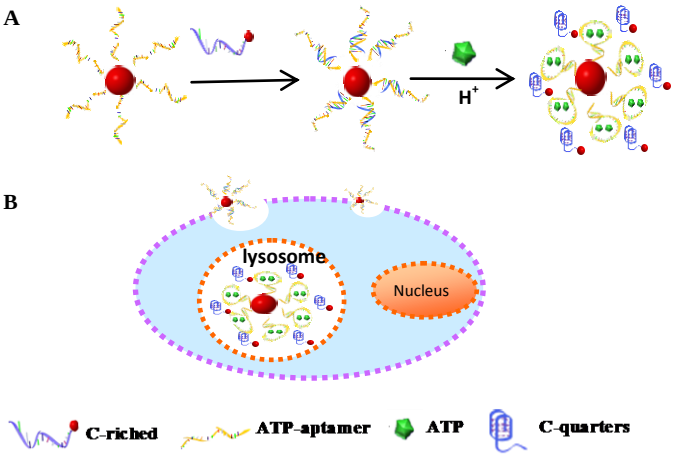

Scheme 1 The schematic illustration of the pH and ATP dual-stimuli triggered disassembly of i-motif/nanoflares (A) in solution and lysosome (B).

In this paper, i-motif is employed to develop a new aptamer nanoflares to achieve lysosome analyte sensing and imaging. Unlike the traditional aptamer nanoflares,[8] it can detect intracellular ATP but cann't localize subcelluar such as specifically in lysosomes and monitor lysosomal ATP. In our design, combinding TAMRA-labeled i-motif domain reporter strand but not a short complementary Cy5-labeled reporter strand, it can localize subcelluar lysosome. Our aptasensor is sensitive to pH, colocalization study with commercial available lysotrackers shown it can sense ATP in lysosome. The fluorophore labled reporter strand containing a DNA i-motif domain, cooperative effect between low pH value in lysosome and the analytes can cause a conformational change and result in a new folded secondary structure. This folded structure disrupts the Watson-Crick base-pairing between the aptamer and the flare, which causes the flares to be liberated with an increase in fluorescence in lysosome due to the greater distance of the flare from the gold surface. So as to localize in cellular lysosome, i-motif sequence is used to assemble DNA-functionalized gold nanoparticles through DNA hybridization, to improve the stability

within a cellular environment, we added several nucleic acids bases to ATP-aptamer and hybridize to i-motif DNA with a certain stability within a cellular environment. We considered all the factors and designed the DNA sequence (shown in ESI†)carefully. Adenosine triphosphate (ATP), best known for its roles in energy metabolism, intracellular signalling, biosynthetic reactions and active transport, is a crucial extracellular signalling molecule.[9] It has been reported that the presence of ATP can accelerate lysosomal disruption and thereby stimulates proteolysis.[10] Therefore, using our constructed aptamer nanoflares for visualization of the distribution and concentration of ATP in lysosome would be very important and helpful to elucidate the biological roles of ATP.

As proof-of-concept, as shown in Scheme 1, this new aptamer nanoflares were designed with several features that make them well suited for ATP detection under acidic condition. 13 nm AuNPs were prepared and characterized according to the reported method[11] and transmission electron microscopy (TEM) shows a size distribution of the attained AuNPs from 10 to 15 nm, most being 13 nm (Fig. S1†). Thiolated ATP aptamer sequence (P1, sequences shown in ESI†) was conjugated to the AuNPs via gold-thiol bond. UV-visible spectroscopic measurement was performed to monitor the change of the nanoparticle in the solution (Fig. S2†). To minimize the contribution from dye fluorescence variation at different pHs, carboxytetramethylrhodamine (TAMRA), a red fluorescent dye whose fluorescence is insensitive to pH in range 4-10,[12] is used, lysosomes that contain a lot of acid hydrolases in the pH range from 4.5 to 6.0,[7] thus TAMRA fluorescence is affected by acidic pH in the lysosomes can be ignored. ATP didn't quench the fluorescence of TAMRA even when the concentration of ATP reached 2 mM (Fig. S3†). A short TAMRA dye-terminated reporter sequences (P2, sequences shown in ESI†) containing DNA i-motif domain hybridizes with P1 capable of acting as "flares" which can be displaced by analyte under specific condition. In the bound state (pH 7.4 and pH 5.2), as demonstrated in Fig. 1A (curve a and curve c, respectively). The TAMRA fluorescence of P2 is quenched due to proximity to the AuNPs surface. Upon addition of 2 mM ATP to the pH 7.4 buffer solution, fluorescence enhancement still can't be observed (Fig. 1A, curve b). This is mainly because P1/ATP binding cannot disassemble the long complementary structure between P1 and P2. As for the pH 5.2 buffer solution, as shown in curve d in Fig. 1A, we can see that the fluorescence emission is increased to 455% after 2 mM ATP addition. In this case, high concentration of H^+ and ATP both served as triggers to disassemble the complex P1/P2, the flare strand P2 is displaced and liberated from the AuNPs by forming the longer and more stable duplex between ATP and the P1-modified AuNPs. It responds rapidly to its target molecules, exhibiting saturated or near saturated signaling within 6 min of the addition of their targets(Fig. S4†), it can realize real-time ATP sensing.

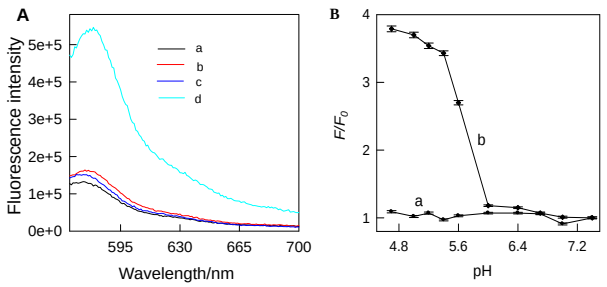

Fig. 1 (A) Fluorescence emission spectra of the dual-stimuli aptamer nanoflares under different conditions. (a), in pH 7.4 buffer (—); (b), a) + 2.0 mM ATP (—); (c), in pH 5.2 buffer (—); and (d), c) + pH 2.0 mM ATP (—). (B): pH-dependent fluorescence change of the aptamer nanoflares in the absence (curve a) and presence of 2.0 mM ATP (curve b). The concentration of aptamer nanoflares is 30 nM. λex/λem = 560 nm/580 nm)

To further investigate the contribution from pH variation in the absence of ATP, F/F_0 of our constructed nanoflares were attained under different pH (from 7.4 to 4.5) and the value kept mostly unchangeable, as shown in Fig. 1B (curve a), where F_0 and F are the TAMRA fluorescence intensities at 580 nm in the absence and the presence of ATP, respectively, suggesting no P2 release due to the i-motif formation here cann't compete with P1/P2 base pairing. We further reduce the pH value in the buffer solution which contained 2 mM ATP. As pH was decreased further, a sharp increase of F/F_0 was seen at about pH 5.2 and quickly reached saturation (Fig. 1B, curve b), suggesting efficient release of P2. For control experiments, non-ATP binding aptamer/i-motif on gold nanoparticle was tested the effect of pH(Fig. S5†) and ATP(Fig. S6†) on such an architecture, fluorescence didn't quenched. These results thus demonstrate that our nanoflares are efficient in signaling the presence of a specific molecule under low pH which has potential application of ATP sensing in lysosome.

To demonstrate the applicability of the proposed aptamer nanoflares in terms of the quantitative fluorescent detection of ATP under acidic condition (pH 5.2), we measured the fluorescence emission spectra of aptamer nanoflares in the sodium phosphate buffer containing ATP at varying concentrations. As shown in Fig. 2A, no observable TAMRA emission appeared when ATP was absent. However, upon the addition of ATP to the solution, significant TAMRA emission at 580 nm was realized. The intensity of the fluorescence increased in proportion to the amount of ATP in the solution, i.e., from 0.05 to 3.0 mM. ATP is present in low concentrations (<0.4mM) in the extracellular environment, but is relatively concentrated within the intracellular cytosol (1-10mM);[13] thus, our aptamer nanoflares were able to sensitively respond to intracellular ATP expression. The specificity of this aptamer nanoflares was tested by introduction of analogues of ATP, including cytosine triphosphate (CTP), thymidine triphosphate (TTP), guanidine triphosphate (GTP), and uridine triphosphate (UTP). Results showed that other analogues could not induce any obvious change in the fluorescence, even with a high concentration (Fig. 2B). The good selectivity and sensitivity of the aptamer nanoflares predicted its potentially applicable in ATP imaging in lysosome.

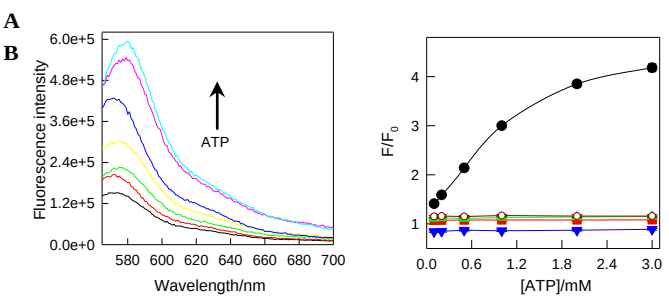

Fig. 2 (A) Fluorescence emission spectra of the aptamer nanoflares in the presence of increasing amounts of ATP. The arrow indicates the signal changes as increases in ATP concentrations (0, 0.05, 0.1, 0.5, 1, 2 and 3 mM ATP). (B) F/F_0 of the in the sodium phosphate buffer by increasing concentrations of ATP(●), CTP (■), GTP (▲), UTP(▼) and analogues (○), separately. F_0 and F are the fluorescence at 580 nm of the nanoflares in the absence of ATP, respectively. pH=5.2 and the concentration of aptamer nanoflares is 30 nM. λex/λem= 560 nm/580 nm)

Having demonstrated the signaling ability of the aptamer nano-flares in solution, to further explore the application of the aptamer nanoflares in living cell imaging, we carried out the colocalization study with commercial available lysotrackers and incubated with cells to determine the specificity in intracellular localization. Cells were cultured on slide chambers, incubated with aptamer nanoflares, and imaged using scanning confocal microscopy. As shown in Fig. 3A, when the mono-emission mode imaging was used; the aptamer nanoflares incubated cells showed a bright densely punctuated pattern in the cytoplasm which is attributed to the fluorescence recovery of liberated flare probe P2, and the cells which wasn't incubated showed only a dim background. With the post-incubation time increased from 1.0 to 3.0 h, the red spots were observed to be increased. Simultaneously, to further confirm the cellular distribution of the red spots assuredly caused by the presence of ATP in lysosome, colocalization of aptamer nanoflares and lysosomes was examined by co-staining LysoTracker Green. The observed yellow colocalization areas of the red fluorescence from aptamer nanoflares and the green fluorescence from LysoTracker Green also exhibited an increasing trend, which indicated a gradual accumulation of aptamer nanoflares into the lysosomes of Hela cells. The further quantification of colocalization efficiency has revealed that there was a time-dependent enhancement of Pearson's coefficient from 0.252 ± 0.052 in 1 h to 0.551 ± 0.112 in 3 h (Fig. 3B, Fig. S7†). However, the colocalization efficiency did not continue to increase by furtherly prolonging the post-incubation time to 6 h, pearson's coefficient is 0.575±0.093. However, the fluorescence decreased when incubation overtime, Pearson's coefficient is 0.183 ± 0.112 in 10h incubation (Fig. S8†). Therefore, it was considered that the post-incubation time of 3 h was sufficient to achieve the perfect sensing and imaging ATP in lysosome.

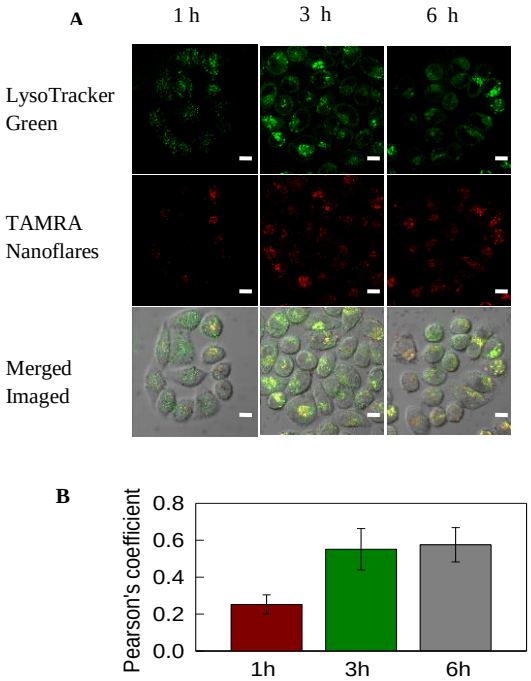

Fig. 3 (A) Laser sanning confocal microscopy images of Hela cells that were incubated with 30 nM TAMRA-aptamer nanoflares for 1.0, 3.0, and 6.0 h, respectively. The scale bar is 10 μm. (B) Analysis of fluorescence colocalization. Pearson's coefficient ± standard deviation (n=6) for the colocalization of TAMRA-aptamer nanoflares with LysoTracker Green fluorescence was obtained with Image J.

Finally, to study the ability of this designed aptamer nanoflares to respond to changes of ATP expression in lysosome, we used two small molecules, etoposide and oligomycin, to stimulate or suppress the expression level of intracellular ATP in living Hela cells, respectively.[4e] Hela cells were first treated with either 100 μM etoposide or 3 μg/mL oligomycin, followed by culturing with ATP aptamer nanoflares. The confocal results indicate that cells treated with epotoside exhibited increased fluorescence signal compared to untreated Hela cells, while cells treated with oligomycin showed decreased cell-associated fluorescence (Fig. S9†). It can be concluded that our constructed aptamer nanoflares could be used as an effective indicator for the application of lysosome-related real-time ATP sensing. Our nanoflares exhibited survival rates close to 100% after incubation for 24 h or 48 h (MTT assay in Fig. S10†), suggesting low cytotoxic effects of our aptasensor.

Conclusions

In summary, we present herein a new aptamer nanoflares which is sensitive to physiologically relevant changes in ATP concentrations in acidic environment. This dual-triggered strategy shows high selectivity for ATP under acidic condition. Only low pH and presence of ATP can lead to the releasing of the flares probe and "light up" the fluroscence of these aptamer nanoflares. The successful application of our aptamer nanoflares to sense and detect lysosomal ATP will help to study the biological role of ATP in lysosomes. Given that similar nanoconjugates can be prepared with a variety of nucleic acid aptamers, thus can be extended for detecting a range of other analytes based on aptamer binding in lysosome and encourage the appearance of new probes suitable for other organelle localizations. Our technique opens a new avenue in sensing and quantifying subcellular level signaling molecule and improve our understanding of subcellular signaling and function.

Acknowledgements

The work was supported by National Natural Science Foundation of China (21135001, 21305036, 21221003, and J1103312), and the ''973''National Key Basic Research Program (2011CB91100-0).

Notes and references

[a] State Key Laboratory of Chemo/Biosensing and Chemometrics, College of Chemistry and Chemical Engineering, Hunan University, Changsha, 410082, P. R. China.†
[b] Hubei Key Laboratory of Mine Environmental Pollution Control & Remediation, Environmental Science and Engineering College, Hubei Polytechnic University, Huangshi, 435003, P. R. China. Fax/Tel: (86)731-88822523;E-mail: Yangrh@pku.edu.cn
†Electronic Supplementary Information (ESI) available: Experimentsand other mentioned data. See DOI: 10.1039/b000000x/

1 D. G. Spiller, C. D. Wood, D. A. Randa and M. R. H. White, *Nature* 2010, **465**, 736 – 745.
2 (a) D. Srikun, A. E Albers, C. I. Nam, A. T. Iavarone and C. J. Chang, *J. Am. Chem. Soc.* 2010, 132, 4455-4465; (b) M. Kamiya and K. Johnsson, *Anal. Chem.* 2010, 82, 6472-6479; (c) E. Tomat, E. M. Nolan, J. Jaworski and S. J. Lippard, *J. Am. Chem. Soc.* 2008, 130, 15776-15777.
3 (a) C. S. Lim, G. Masanta, H. J. Kim, J. H. Han, H. M.Kim and B. R. Cho, *J. Am. Chem. Soc.* 2011, **133**, 11132-11135; (b) G. Masanta, C. S. Lim, H. J. Kim, J. H. Han, H. M. Kim and B. R. Cho, *J. Am. Chem. Soc.* 2011, **133**, 5698-5700; (c) S. C. Dodani, S. C. Leary, P. A. Cobine, D. R. Winge and C. J. Chang, *J. Am. Chem. Soc.* 2011, **133**, 8606-8616; (d) B. C. Dickinson and C. J. Chang, *J. Am. Chem. Soc.* 2008, **130**, 9638-9639; (e) Y.

Kurishita, T. Kohira, A. Ojida and I. Hamachi, *J. Am. Chem. Soc.* 2012, **134**, 18779−18789.
4 (a) S.Tyagi, D. P.Bratu, and F. R.Kramer, *Nat. Biotechnol.* 1998, **16**, 49 – 53; (b) J. J. Li, X. Fang, S. M. Schuster, and W. Tan, *Angew. Chem., Int. Ed.* 2000, **39**, 1049 – 1052; (c) D. P. Bratu, B. J. Cha, M. M. Mhlanga, F. R. Kramer, and S. Tyagi, *Proc. Natl. Acad. Sci.* 2003, **100**, 13308 – 13313; (d) K. Wang, Z. Tang, C. J. Yang, Y. Kim, X. Fang, W. Li, Y. Wu, C. D. Medley, Z. Cao and J. Li, *Angew. Chem., Int. Ed.* 2009, **48**, 856 – 870; (e) C. C. Wu, T. Chen, D. Han, M. X. You, L. Peng, S. Cansiz, G. Z. Zhu, C. M. Li, X. L. Xiong, E. Jimenez, C.Y. James Yang and W. H. Tan, *ACS Nano*, 2013, **7**, 5724 – 5731; (f) Z. Li, S. Q. Wu, J. H. Han, and S. F. Han, *Analyst*, 2011, **136**, 3698-3706; (g) C. X. Wang, Y. Du, Q. Wu, S. G. Xuan, J. J. Zhou, J. B. Song, F. W. Sha and H. W. Duan, *Chem Comm*, 2013, **49**, 5739–5741.
5 C. H. Kang, I. Berger, C. Lockshin, R. Ratliff, R. Moyzis and A. Rich, *Proc. Natl. Acad. Sci.*, 1994, **91**, 11636–11640.
6 S. Kendrick, Y. Akiyama, S. M. Hecht, and L. H. Hurley, *J. Am. Chem. Soc.* 2009, **131**, 17667–17676.
7 C. A. Smith and E. J. Wood, In Cell Biology, 2nd ed; Chapman & Hall: London, 1996.
8 D. Zheng, D. S. Seferos, D. A. Giljohann, P. C. Patel, and C.A. Mirkin, Nano lett., 2009, **9**, 3258–3261.
9 (a) G. Burnstock, *Purinergic nerves. Pharmacol. Rev.* 1972, **24**, 509–581; (b) M. Hattori and E. Gouaux, *Nature*, 2012, **485**, 207–212; (c) S. Przedborski and M. Vila, *Clin. Neurosci. Res.* 2001, **1**, 407–418; (d) M. C. Zhao, M. Wang, H. J. Liu, D. S. Liu, G. X. Zhang, D. Q. Zhang and D. B. Zhu, *Langmuir*, 2009, **25**, 676–678; (e) W. Subasinghe, D. M. Spence, *Anal Chim Act.* 2008, **618**, 227–233.
10 W. Huisman, J. M. W. Bouma, and M. Bruber, *Nature*, 1974, **250**, 428–429.
11 R. C. Mucic, J. J. Storhoff, C. A. Mirkin, and R. L. Letsinger, *J. Am. Chem. Soc.*1998, **120**, 12674–12675.
12 T. Li and M. Famulok, *J. Am. Chem. Soc.* 2013, **135**, 1593−1599.
13 R. Mo, T. Jiang, R. DiSanto, W. Tai and Z. Gu, Nat. Commun. 2014, **5**, 3364.